

A Comparative Study of the Aerodynamic Performance of Bridge Sections using CFD.

Breno Tavares de Godoy^{1,2}, Alexandre Magno Lima Cardoso², Osvaldo Shigueru Nakao¹, Rui

Nobhiro Oyamada^{1,2}, Fernando Akira Kurokawa¹

¹ Escola Politécnica da USP / breno.godoy@usp.br

² OUTEC Engenharia Ltda / rui.oyamada@outec.com.br

Abstract

Advances in civil engineering make it possible to build bigger and slender constructions. As a result, conducting detailed analyzes of the interaction between fluids and structures become essential, always aspiring to provide parameters to assist the development of projects. The employment of Computational Fluid Dynamics (CFD) to perform these analyzes has recently boosted based on three pillars: the increase in the computational capacity, the lower costs in comparison with wind tunnel tests and agility in execution. It is important to underline that CFD simulations do not substitute wind tunnel experiments at all. These approaches are complementary.

In this paper, the behavior of different bridge cross sections undergoing wind action were studied through a CFD commercial program in a two-dimensional static approach. The following results were obtained for each geometry studied: the aerodynamic coefficients, the Strouhal number, the velocity fields and the pressure fields.

In order to calibrate the parameters of CFD simulations, a series of experiments were developed. The first one is the flow around a cylinder, to compare the simulation outputs with results found in literature. Subsequently, CFD simulations were executed to analyze two bridges for which were obtained results from wind tunnel tests. In the next stage, another typical bridge section was tested: a girder and slab section. Finally, two studies were presented: the effects of considering or not the guardrails and the influence of fairings in the aerodynamic coefficients.

Key words

CFD, Turbulence, Drag coefficient, Strouhal number, Bridge sections.

Introduction

Since the last century, the civil engineering has faced challenging projects. In this period, long span bridges and enormous skyscrapers were constructed, with groundbreaking geometries and sizes. The following table presents the most notable achievements in the suspension bridge construction scenario.

Table 1 - List of Longest Suspension Bridges [1].

| Name | Country | Span | Year |
|-----------------------------------|---------|-------|------|
| 1 Akashi Kaikyo Bridge | Japan | 1991m | 1998 |
| 2 Yangsigang Yangtze River Bridge | China | 1700m | 2019 |
| 3 Nansha Bridge | China | 1688m | 2019 |
| 4 Xihoumen Bridge | China | 1650m | 2009 |
| 5 Great Belt Bridge | Denmark | 1624m | 1998 |

In order to build these challenging projects, it is crucial to consider its interaction with the wind. Long span bridges are naturally slender and flexible, and for that reason, susceptible to aerodynamic instabilities. These instabilities can cause from small oscillations, which can induce fatigue problems, to huge movements, which can provoke the collapse of the structure.

For that reason, it is necessary to evaluate the fluid-structure interaction. For large projects, wind tunnel tests are essential to analyze the structure, evaluate its aerodynamic coefficients and discover critical velocities. However, wind tunnel tests are expensive experiments that need long periods of time to be done. In this point the CFD simulations can be of great help. It is a tool that can give answers faster, consuming less resources.

Theoretical background: Aerodynamics

The wind falling across a bridge can be seen as an external flow around a bluff body. To make this approach clearly stated, in the next paragraphs some variables and dimensionless parameters are defined, as well as some simplifications and definitions (MUNSON, 2004).

In this study, the fluid is well characterized by its specific mass and its dynamic viscosity. The obstacle is considered a static body in the flow. The wind velocity used in this analyzes is evaluated in a place distant from the obstacle, and can be called non-perturbed velocity. The velocity profile is considered constant when sufficiently distant from the body. This is a premise that not represent the reality of an external wind flow in an open field, but this simplification does not spoil the achievement of results in the region of interest in the model.

The body inside the flow may have a complex geometry, but it's necessary to specify a characteristic dimension to evaluate the dimensionless parameters and the aerodynamic coefficients. The diameter is used as a parameter for the cylinder. In the case of bridge sections, the width (L) of the bridge is used for the Reynolds number and the lift coefficient, and the depth (H) is used for the Strouhal number and the drag coefficient.

Two dimensionless parameters are highlighted. The Reynolds number and the Strouhal number.

The Reynolds Number (Re) is a ratio between the inertial and the viscous forces in a fluid flow. Laminar flows are characterized by low Reynolds numbers ($Re < 1$), and in this case the viscous forces control the phenomenon. In the other hand, elevated Reynolds ($Re > 100$) characterize turbulent flows, where the inertia controls the physics of the system.

The Strouhal number (St) is other relevant dimensionless number in flows around bodies. It is a parameter of the oscillations in the fluid flow that takes place downstream of the obstacle.

Another important definition is the concept of boundary layer. For a flow with a viscid fluid, the relative velocity between a static body in touch with the flow and the fluid is equal to zero in the contact surface. This is the no-slip condition. The boundary layer is a surface where the viscous forces have importance in the vicinity of the body. The velocity profile starts equal to zero in the body and reach the non-perturbed velocity in the end of the boundary layer.

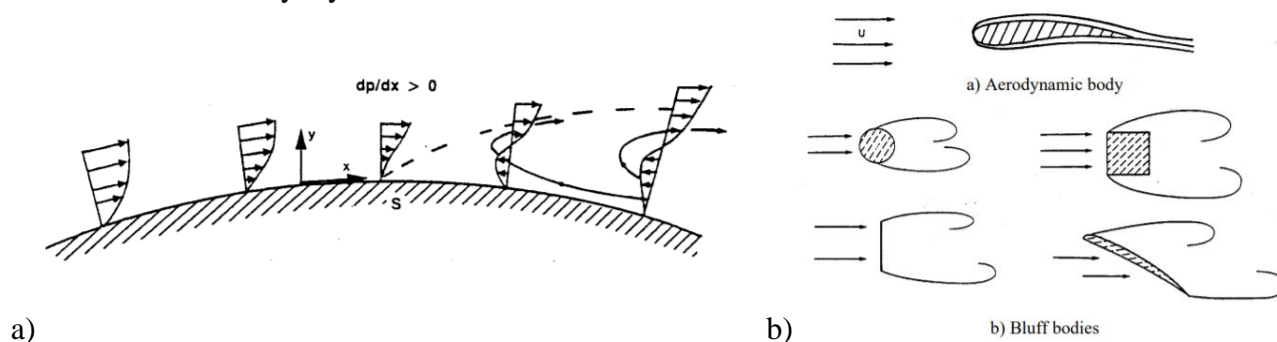


Figure 1 - a) Boundary layer and separation and b) Body shapes. (BURESTI, 2000)

The separation of the boundary layer occurs in a point where, because of the pressure imposed in this region, the particles near the surface suffer a deceleration, changing the velocity profile until occurs a change in the flow direction near the wall, moving upstream. This is the separation point and from this point forward the boundary layer increase, as well as increase the formation of vortices inside this region.

Regarding the body immersed in the flow, it can be a bluff body or a streamlined (aerodynamic) body. The first one is fitted with a geometry that provide a flow separation in the most part of the body, while for the second the separation occurs only for a small part. An example of a bluff body is a cylinder with a square cross section. In the other side, an airplane wing is a streamlined surface. Figure 1 demonstrate that not only the geometry off the body defines the type of flow, but also its orientation related to the flow.

Regarding the geometry of the body, the aspect ratio is the relation between the longitudinal and the transversal length of the structure. An elevated aspect ratio means a slender structure. In structures with this feature, the bi-dimensional analyzes can give satisfactory results.

Considering that long span bridges have high aspect ratios; a two-dimensional approach can be used to investigate the fluid structure interaction in this case. It is necessary to emphasize that using this simplification some important features of the structure like the cables and the diaphragms are ignored. These substructures only can be represented in a three-dimensional model.

Two coefficients are going to be analyzed in this study: the drag coefficient (C_D) and the lift coefficient (C_L).

$$C_D = \frac{2F_D}{D\rho U^2} \quad (1)$$

$$C_L = \frac{2F_L}{D\rho U^2} \quad (2)$$

The lift coefficient is related to the aerodynamic forces imposed on the section in the cross-line direction with the flow, while the drag coefficient is evaluated based on the forces acting against the body in the same direction as the fluid flow. These are two dimensionless numbers related to the shape of the body, but also with an important dependence on the Reynolds number.

Summarizing, the studies developed in this paper consist basically in a static analyzes of a two dimensional external and turbulent flow of a viscous and incompressible fluid around a bluff body.

The objective is to understand how the aerodynamic forces act against this body and visualize the development of the flow around the cross section observed. The velocity fields and the streamlines are obtained. In view of this, it is necessary to choose a mathematical model which makes it possible to achieve these results.

The mathematical model that describes this problem are the well know Navier-Stokes equations associated with the mass conservation equation presented subsequently:

$$\rho \left(\frac{\partial \mathbf{V}}{\partial t} + \mathbf{V} \cdot \nabla \mathbf{V} \right) = -\nabla p + \rho \mathbf{g} + \mu \nabla^2 \mathbf{V} \quad (3)$$

$$\nabla \cdot \mathbf{V} = 0 \quad (4)$$

This is a set of second order nonlinear differential equations to partial derivatives. It is essential to highlight that this system with four equations and four variables (velocity in three directions and pressure) has analytic solution only for specific problems like the laminar flow in permanent regime between parallel plates (MUNSON, 2004, p.312), where the system is hugely simplified.

The flow around the deck of a bridge is characterized by a turbulent flow, in a transient regime involving complex geometries, and all these factors end up with a lack of analytical solutions for this system. In this case, the only solution is to use numerical methods to solve these equations. The computational effort required to solve these algebraic systems depends on the numerical methods chosen.

This leads us to an important topic: the mathematical modeling of turbulence. The turbulence model plays an important role in the simulation and can change enormously the time required to execute the calculations. There are three major classes of turbulence models: Direct numerical simulations (DNS), Large Eddy Simulation (LES) and the Reynolds Averaged Navier Stokes (RANS).

The computational efforts required to solve a problem decreases as the percentage of turbulence modelling increase. Other way round, when the percentage of turbulence modelled increases the right model need to be carefully chosen in order to achieve coherent results. The model selected for this study is the RANS $k - \omega$ SST. Although this model has a high degree of modeling, it presents good adherence to the physical phenomenon of external flows around bluff bodies when compared with other RANS models, and dispense a smaller computational effort when compared with LES models (COSTA, 2018).

Simulation tool and procedures

The simulations presented in this paper were developed using the academic license of Ansys Fluent®, in the versions 2020R1 and 2020R2. In the academic version the maximum number of nodes that can be used is 512000. The simulation procedure can be divided in four steps:

1. design the domain with the obstacle positioned in a central position,
2. build a mesh with a greater refinement near the obstacle and in the street of vortices.
3. Insert parameters to execute the simulation: fluid properties, inlet velocity, obstacle characteristic dimensions. Define the outputs to be evaluated during the calculation, like the drag coefficient and lift coefficient. Specify points to collect data for further analyzes.
4. Execute the post processing, analyzing velocity and pressure fields, streamlines, vortex patterns developed around the body, and the aerodynamic coefficients.

The simulations were executed in a computer equipped with an Intel® Core™ i7-7700 processor with a memory of 16Gb located at LABCAD in Escola Politécnica of USP.

Case I: Circular Cylinder

The first case is a study about the flow around a circular cylinder. This is a classical problem in the fluid-structure field with experimental and numerical data available in literature. For this case, two Reynolds numbers are tested: 40 and 1000. With $Re = 40$, it is expected to observe two stationary symmetric recirculating eddies right behind the cylinder. To demonstrate the behavior expected, pictures of this flow collected by Van Dike (VAN DYKE, 1982) are presented. These are pictures of a cylinder moving through a tank of water containing aluminum powder, illuminated by a sheet of light below the free surface.

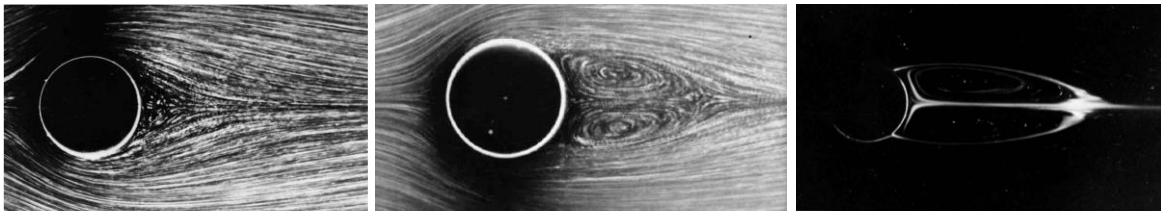


Figure 2 - Flow around a cylinder. In order: $Re = 10$, $Re = 26$ and $Re = 41$ (VAN DYKE, 1982).

To perform this study the following geometry is employed.

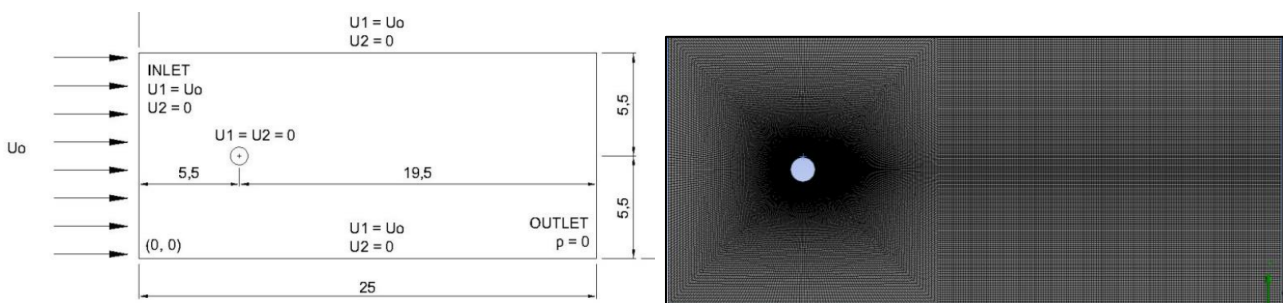


Figure 3 - Domain and boundary conditions (COSTA, 2018). Mesh with 67792 nodes (AUTHOR).

Figure 3 also presents the boundary conditions adopted. Subscript 1 refers to the horizontal direction and subscript 2 refers to vertical direction. The same velocity is employed in the inlet, and in the upper and lower limit of the domain. The no-slip condition is applied in the cylinder limit and in the top and bottom edges of the domain. A structured mesh was elaborated with, 67.792 nodes, applying a great refinement nearby the body, as can be observed in Fig. 3.

Table 2 - Parameters used in the simulation.

| Parameter | Value | Parameter | Value |
|----------------|---------------------|-----------------------------|----------------------|
| Timestep [s] | $1,8 \cdot 10^{-4}$ | Diameter [m] | 1 |
| Duration [s] | 27 | ρ [kg/m ³] | 1,225 |
| Velocity [m/s] | 10 | μ [Ns/m ²] | $3,06 \cdot 10^{-1}$ |

With all this inputs, the simulation was performed. In Fig. 4 can be observed the velocity fields and the streamlines generated. As expected, the formation of two symmetric vortices behind the cylinder can be observed. The drag coefficient obtained is equal to 1,78, the mean value in the steady state.

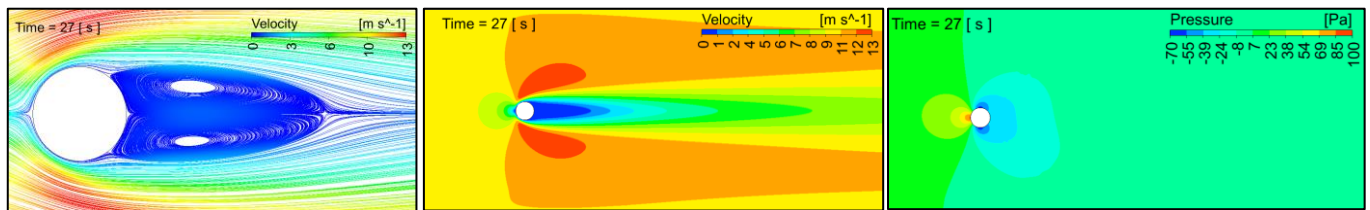


Figure 4 - Streamlines, Velocity field and Pressure field. $Re = 40$.

Another simulation was performed for the same geometry, adopting $Re = 1000$. Figure 5 shows the velocity fields and the streamlines produced. It is possible to note the alternate vortex shedding downstream the flow, as expected for this Re . In Fig. 5 the time story of the aerodynamic coefficients are presented.

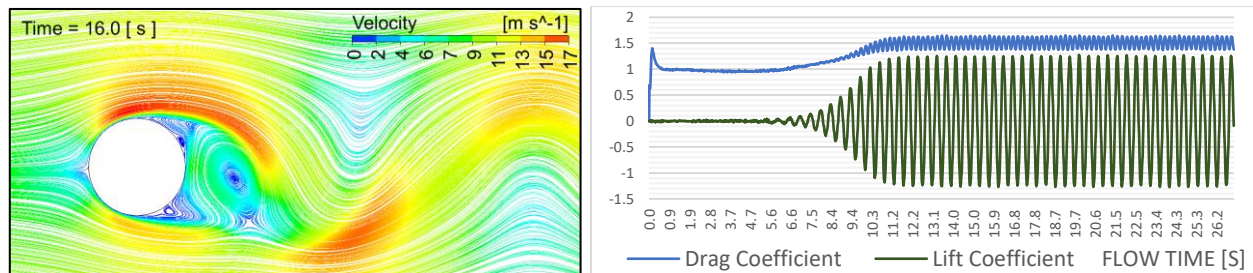


Figure 5 - Velocity field, Streamlines and Aerodynamic Coefficients. $Re = 1000$.

In the next table, results obtained in this study are compared with reference values. There is a good adherence for the drag coefficient. The lift coefficient presents values with a bigger difference when compared with these reference works.

Table 3 - Results.

| Re | Study | C_D | C_L | St |
|------|-------------------------|-------|-------|-------|
| 40 | Present paper | 1,78 | - | - |
| | COSTA, 2018 (Reference) | 1,79 | - | - |
| | BRAUN, 2007 (Reference) | 1,77 | - | - |
| 1000 | Present paper | 1,52 | 1,27 | 0,229 |
| | COSTA, 2018 (Reference) | 1,64 | 1,80 | 0,215 |
| | BRAUN, 2007 (Reference) | 1,62 | 1,82 | 0,217 |

Table 4 - Next simulations parameters

| Parameters | Value | Parameters | Value |
|--------------|---------------------|-----------------------------|-------|
| Timestep [s] | $5,0 \cdot 10^{-4}$ | Velocity [m/s] | 38,00 |
| Duration [s] | 15,00 | ρ [kg/m ³] | 1,225 |

For the next cases some parameters will be maintained for all simulations. These parameters are described in the Table 4.

Case II: Cidade de Guarulhos Bridge.

The first bridge analyzed is located in Guarulhos (São Paulo, Brazil). It is a cable-stayed bridge with a total length of 170m, and one pillar 60m high. The concrete deck is supported by a central cable plane and the typical cross section has a trapezoidal box shape.

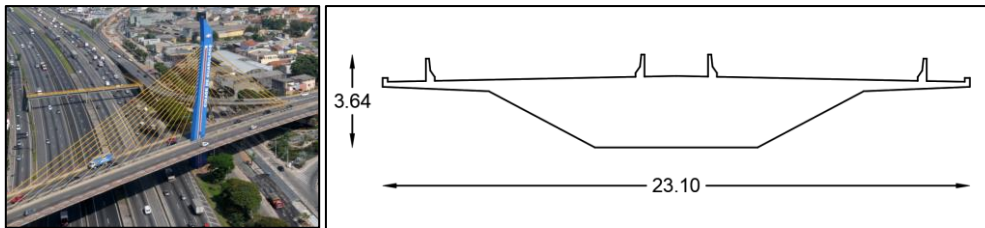


Figure 6 - Viaduct Cidade de Guarulhos. Cross section.

The values obtained with the simulation in this work will be compared with the results from a wind tunnel test developed by *Laboratório de Aerodinâmica das Construções* from *Universidade Federal do Rio Grande do Sul*. The Reynolds number employed in the wind tunnel experiment for the evaluation of the aerodynamic coefficients is 1.000.000, and this value was employed in the CFD approach.

The geometry developed for the simulation is presented in Fig. 7. For the next cases the same position of the section in the domain will be used. Regarding the mesh, the same strategy will be used in the subsequent simulations. Two regions are going to be more refined: a circle around the section and the street of vortices.



Figure 7 - Section into the CFD domain and mesh with 134.308 nodes.

Table 5 - Parameters used in the simulation.

| Parameters | Width [m] | Depth [m] | μ [Ns/m ²] |
|------------|-----------|-----------|----------------------------|
| Value | 23,1 | 3,64 | 1,08.10 ⁻³ |

Although, on a preliminary inspection, this geometry can be considered streamlined, the simulation shows a series of recirculating vortices among the guardrails and also recirculating vortices at the lower part of the cross section. Following the results: velocity field, streamlines and the aerodynamic coefficients.

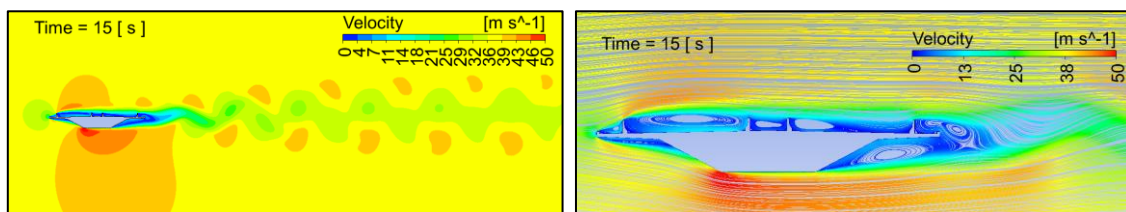


Figure 8 - Velocity field and streamlines with vortices.

The results are compared with the values presented in the wind tunnel report. There is an adherence between the results. It is important to underline that the wind tunnel is a tri-dimensional experiment and this CFD simulation is a two-dimensional study. Taking it into consideration, some differences are acceptable.

Table 6: Results.

| Study | C_D | C_L | St |
|---------------|-------|-------|-------|
| Present paper | 0,54 | -0,23 | 0,201 |
| Wind tunnel | 0,63 | -0,11 | - |

Case III: Governador Orestes Quercia Bridge.

The second bridge analyzed is located in São Paulo (São Paulo, Brazil). It is a cable stayed bridge with a total length of 660m and a main pylon 55m high. This bridge has two cable planes to support a concrete girder-slab section. The typical cross section geometry is presented below.

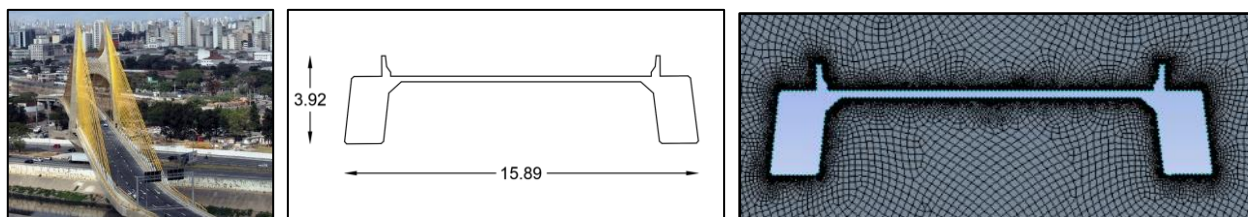


Figure 9 - Governador Orestes Quercia cable stayed bridge and the typical cross section.

The mesh developed for this case has 129350 nodes. For this bridge there is also a wind tunnel test available. In this case, the experiment was developed by *Laboratório de Sistemas Estruturais LTDA*. The wind tunnel from *Instituto de Pesquisas Tecnológicas do Estado de São Paulo* was used to perform the experiment. The Reynolds number for this problem is 300.000. The main parameters for the simulation are presented below.

Table 7 - Parameters used in the simulation.

| Parameters | Width [m] | Depth [m] | μ [Ns/m ²] |
|------------|-----------|-----------|----------------------------|
| Value | 15,89 | 3,92 | 2,46.10 ⁻³ |

The results obtained for this deck is presented in the sequence. For this cross section an alternating vortex shedding can be observed downstream as well as recirculatory eddies, in the upper side of the section between the guardrails, and between the girders in the lower part.

A comparison between the CFD and the wind tunnel test are done in the following table.

Table 8 - Results.

| Study | C_D | C_L | St |
|---------------|-------|-------|-------|
| Present paper | 0,87 | -0,26 | 0,162 |
| Wind tunnel | 1,02 | -0,12 | - |

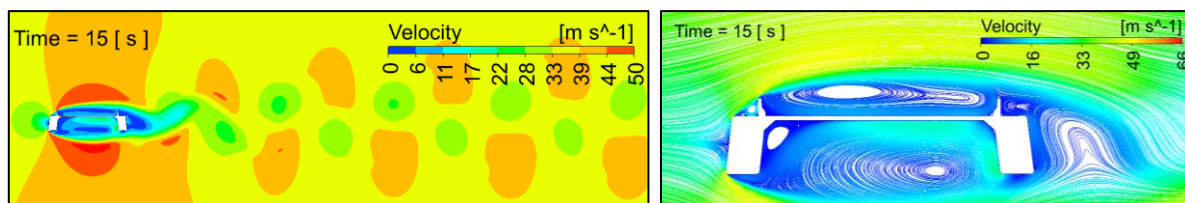


Figure 10 - Streamlines and velocity field.

Case IV: concrete girder-slab section

The next typical bridge section studied is a common solution adopted for small bridges. This section consists of a concrete slab with a number of longitudinal girders and the guardrails. This model is widely used for small spans, between 20 and 40 meters. The major interest in this case is evaluate the drag coefficient and make a comparison with drag coefficients presented in the Brazilian wind code, the NBR 6123.

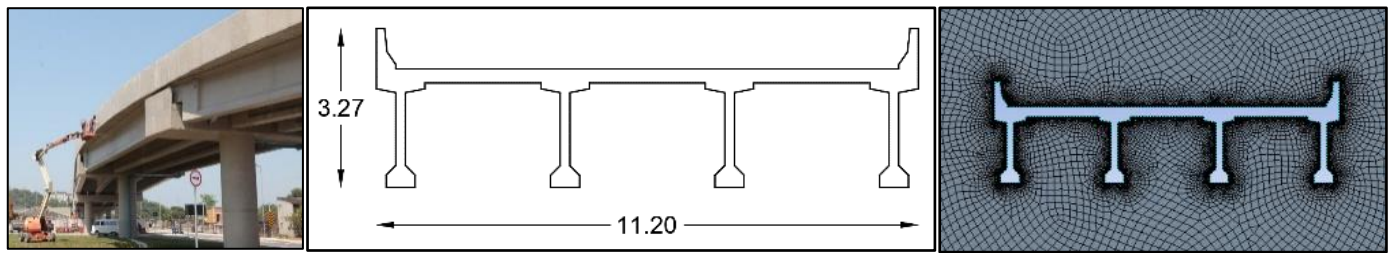


Figure 11 - Girder-Slab bridge photo [2], cross section and mesh developed.

The mesh developed for this case has 131.182 nodes. The parameters used are in the following table.

Table 9 - Parameters used in the simulation.

| Parameters | Width [m] | Depth [m] | μ [Ns/m ²] |
|------------|-----------|-----------|----------------------------|
| Value | 11,20 | 3,27 | $1,74 \cdot 10^{-3}$ |

The streamlines presented bellow demonstrate a turbulent flow with a considerable number of eddies on the bottom and the top side of the section.

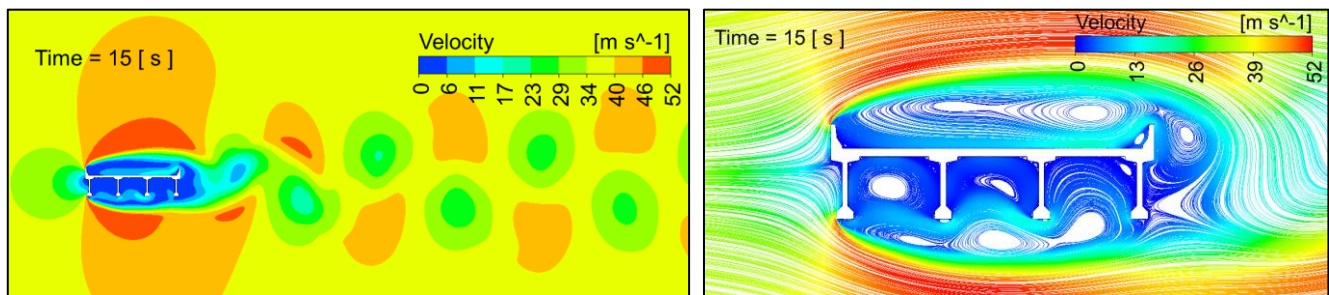


Figure 12 - Streamlines (section with guardrails).

There is no specific values for bridge cross sections in NBR 6123. The value used in order to do a comparison is the rectangular shape with the ratio between width and depth equal to 0.5, and the aspect ratio tending to infinite. This value is obtained in Table 10 of NBR 6123.

Table 10 - Results.

| | This study | NBR 6123 |
|-------|------------|----------|
| C_D | 1,20 | 0,70 |

Case V: Guardrails Influence (GR)

In cases V and VI, studies are carried out on the impact that some elements can have on the aerodynamic behavior of the cross sections. In the first study, the presence of the guardrails is analyzed in *Cidade de Guarulhos Bridge*. The Reynolds number employed in this study is 300.000.

Table 11 - Parameters used in the simulation.

| Parameters | Width [m] | Depth [m] | μ [Ns/m ²] |
|------------|-----------|-----------|----------------------------|
| With GR | 23,10 | 3,64 | $3,58 \cdot 10^{-3}$ |
| Without GR | 23,10 | 2,80 | $3,58 \cdot 10^{-3}$ |

The section with the presence of the guardrails is characterized by a number of recirculating vortices between these elements while for the section without guardrails a flow much less disturbed takes place in this region. The bottom side of the bridge has a similar pattern for both cases, although the recirculating eddies are smaller in the section without guardrails. In both cases, for $Re = 300.000$, the vortex shedding cannot be observed.

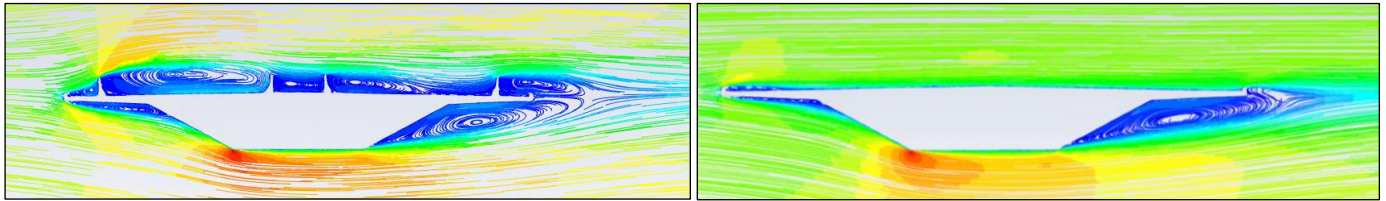


Figure 13 - Streamlines: with GR and without GR.

An important change can be observed in the aerodynamic coefficients and in the entire flow as the guardrails are vertical obstacles that change abruptly the wind direction causing the separation of the flow and a series of recirculating zones in the top side of the section. Table 12 presents the mean value in the stationary segment of the aerodynamic coefficients chart.

Table 12 - Results for $Re = 300.000$.

| Study | C_D | C_L |
|------------------------|-------|-------|
| With the guardrails | 0,50 | -0,26 |
| Without the guardrails | 0,38 | -0,34 |

Case VI: Aerodynamic Countermeasures: Fairings

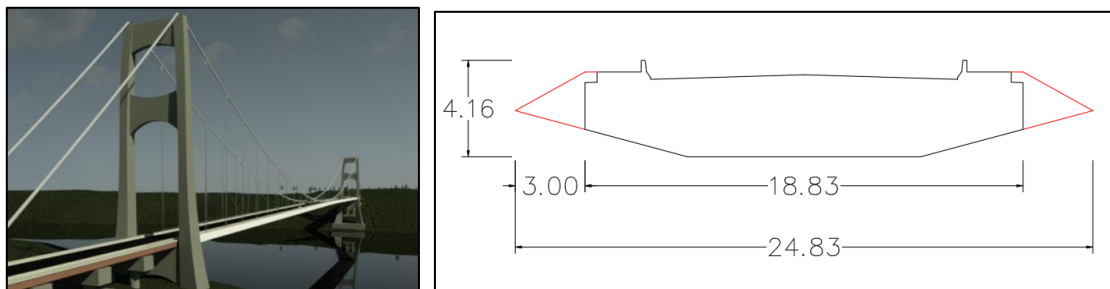


Figure 14: Bridge project and bridge cross section.

The last study presented is a comparison between the performance of a single cell box cross section with and without fairings. This study was developed for the *2º Concurso CBCA para Estudantes de Engenharia*, where a group of civil engineering students developed a project of a cable supported bridge to connect Brazil to Paraguay. The optimization of the section was one of the studies developed by the author for this project. Figure 14 shows a tri-dimensional view of the bridge and the section with the fairings in red. The Reynolds employed in this study is 300.000.

Table 13 - Parameters used in the simulation.

| Parameters | Width [m] | Depth [m] | μ [Ns/m ²] | Mesh |
|------------------|-----------|-----------|----------------------------|---------------|
| With fairings | 24,83 | 4,16 | $4,87 \cdot 10^{-3}$ | 100.426 nodes |
| Without fairings | 18,83 | 4,16 | $3,69 \cdot 10^{-3}$ | 97.297 nodes |

Figure 15 shows the velocity fields for these sections. One can note that the absence of fairing makes the flow much more disturbed, with a more intense release of vortices. Results in Table 14 shows the impact in the aerodynamic coefficients.

Table 14 - Results for $Re = 300.000$.

| Study | C_D | C_L | St |
|----------------------|-------|-------|-------|
| With the fairings | 0,34 | -0,48 | 0,315 |
| Without the fairings | 0,46 | -0,60 | 0,244 |

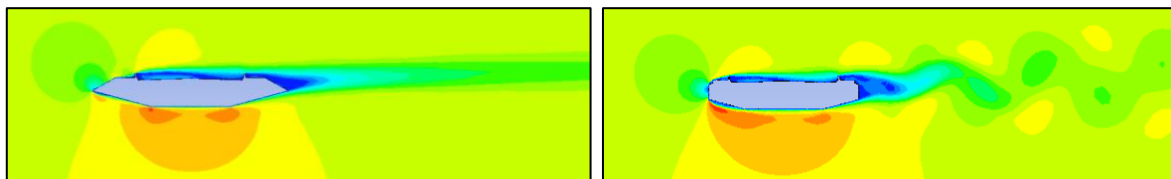
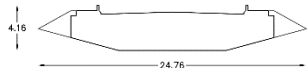
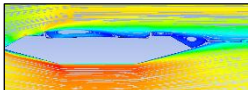

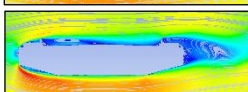
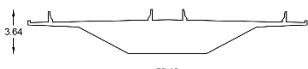
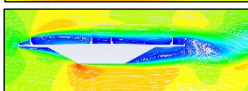

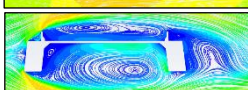

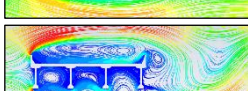


Figure 15 - Velocity field.

Concluding remarks

Achieve values for the aerodynamic coefficients of the bridge cross sections can be an important contribution of the CFD simulations. The main objective of this paper is to analyze some of the most common sections regarding their aerodynamic behavior, always comparing the results with reference values, from wind tunnel tests to results found in literature. Some elements introduced in the geometry incurred in deep changes in the flow pattern and in the aerodynamic coefficients, demonstrating the importance of taking these elements into account when performing CFD analyzes. The following table shows the drag coefficient for some sections found in this paper.

Table 15 - Sections, C_D and streamlines.

| Cross Sections | Streamlines | C_D |
|---|---|-------|
|  |  | 0,34 |
|  |  | 0,46 |
|  |  | 0,50 |
|  |  | 0,87 |
|  |  | 1,20 |

Acknowledgments

Special thanks to *Outec Engenharia LTDA* for providing the two wind tunnel test reports used in this paper.

References

- MUNSON, B. R.; YOUNG, D. F.; OKIISHI, T. H. Fundamentos da mecânica dos fluidos. Translated from the fourth American version: Euryale de Jesus Zerbini. – São Paulo: Blucher, 2004.
- BURESTI, G. Bluff-body aerodynamics. Lecture Notes, University of Pisa, Italy, 2000.
- COSTA, L. M. F. Investigação numérica de modelos de turbulência no escoamento do vento em pontes suspensas. 2018. Dissertação (Mestrado) – Escola Politécnica da Universidade de São Paulo, 2018.
- VAN DYKE, M. Album of Fluid Motion. California: The Parabolic Press, 1982.
- BRAUN, A. L. Simulação numérica do vento incluindo efeitos de interação fluido-estrutura. 2007. Tese (Doutorado). Universidade Federal do Rio Grande do Sul, 2007.
- ASSOCIAÇÃO BRASILEIRA DE NORMAS TÉCNICAS. NBR 6123: Forças devidas ao vento em edificações. Rio de Janeiro: ABNT, 1988.
- [1] Available in: https://en.wikipedia.org/wiki/List_of_longest_suspension_bridge_spans. Access: Dec. 03, 2020.
- [2] Available in: <https://www.santos.sp.gov.br/?q=noticia/ponte-são-jorge-e-avenida-beira-rio-na-zona-noroeste-recebem-arremates-finais>. Access: Dec. 03, 2020.